

Convective Entrainment and Large-Scale Organization of Tropical Precipitation: Sensitivity of the CNRM-CM5 Hierarchy of Models

BOUTHEINA OUESLATI AND GILLES BELLON

Centre National de Recherches Météorologiques, Centre National de Recherches Scientifiques/Météo-France, Toulouse, France

(Manuscript received 4 June 2012, in final form 8 November 2012)

ABSTRACT

The spurious double intertropical convergence zone (ITCZ) is a systematic bias affecting state-of-the-art coupled general circulation models (GCMs). Modeling studies show that the ITCZ structure is very sensitive to moist convection parameterization and in particular, to the vertical profile of convective heating and free-tropospheric moistening. To further explore this sensitivity, the authors focus in this study on the influence of lateral entrainment in convective plumes on the simulated tropical precipitation and large-scale circulation. Sensitivity studies to the entrainment parameter were performed in a hierarchy of models (coupled ocean–atmosphere GCM, atmospheric GCM, and aquaplanet GCM), in order to mitigate the double ITCZ problem in the Centre National de Recherches Météorologiques Coupled Global Climate Model, version 5 (CNRM-CM5). The sensitivity of the ITCZ structure to lateral entrainment is robust across our hierarchy of models. In response to increased entrainment, the realistic simulations exhibit a weakening of the southern side of the double ITCZ over the southeastern Pacific Ocean and a better representation of the South Pacific convergence zone (SPCZ). However, as a result of stronger moisture–convection feedbacks, precipitation is overestimated in the center of convergence zones. The change in ITCZ configuration is associated with a more realistic representation of the large-scale vertical regimes, explained by a decreased frequency of weak-to-moderate ascending regimes and an enhanced frequency of subsidence regimes. Mechanisms at play in this circulation change are examined by analyzing the vertically integrated dry static energy budget. This energetic analysis suggests that the feedback between large-scale dynamics and deep convection is crucial in controlling the probability distribution function (PDF) of midtropospheric vertical wind. This PDF, in turn, controls the precipitation distribution and, in particular, the double ITCZ bias.

1. Introduction

General circulation models (GCMs) still present major difficulties in simulating tropical precipitation patterns and variability. In particular, the so-called double intertropical convergence zone (ITCZ) syndrome is one outstanding problem in coupled ocean–atmosphere GCMs (Mechoso et al. 1995; Dai 2006). This bias appears as two persistent, parallel belts of maximum precipitation straddling the equator over the central and eastern Pacific Ocean, whereas this double ITCZ structure is only observed over the eastern Pacific during boreal spring (Hubert et al. 1969). It is associated with a poor simulation of the South Pacific convergence zone (SPCZ),

a precipitation region extending southeastward from the west Pacific warm pool. The double ITCZ bias is also associated with an equatorial cold tongue of sea surface temperature (SST) extending too far to the west in the Pacific that is, in some cases, too cold. Although atmospheric models are believed to be the core causes of the double ITCZ bias (Schneider 2002), coupled ocean–atmosphere feedbacks amplify it, through erroneous representation of the SST–wind-induced surface fluxes feedback, the SST–stratus feedback, and the SST gradient–trade wind feedback associated with vertical upwelling (Lin 2007).

Modeling studies emphasized the role of atmospheric mechanisms in controlling the ITCZ location. Early studies proposed the near-equatorial dynamics to understand the ITCZ location based on the conditional instability of the second kind (CISK) theory (Charney 1971) and the associated wave–CISK mechanisms (Holton et al. 1971; Lindzen 1974; Hess et al. 1993).

Corresponding author address: Boutheina Oueslati, CNRM, CNRS/Météo-France, 42 Avenue Gaspard Coriolis, 31057 Toulouse CEDEX 01, France.
E-mail: boutheina.oueslati@meteo.fr

Waliser and Somerville (1994) argued that convection occurs in the latitude range of about 4° – 12° away from the equator, because of the enhanced feedback between the midtropospheric latent heating and the low-level convergence of moist static energy at these latitudes. Numaguti (1993) highlighted the importance of the distribution of evaporation and the associated wind–evaporation feedback on the tropical precipitation. Under the condition of globally and temporally uniform SST and solar insolation angle, Chao and Chen (2004) attributed the ITCZ location to a balance between the competing contributions of frictional convergence and surface fluxes. A recent study by Oueslati and Bellon (2013) emphasized the role of the low-level convergence in the control of the location of the ITCZ in two state-of-the-art GCMs. Although the general behavior of these models is similar to that expected from CISK, the mechanisms at play are different from those in CISK. In fact, the SST influences the ITCZ location through its forcing of low-level dynamics [via the atmospheric boundary layer (ABL) temperature gradients created by the surface sensible heat flux] rather than by forcing local convection via the surface flux of moist static energy (Charney 1971). Model-dependent dry and moist feedbacks intervene to reinforce or weaken the effect of the surface forcing. In addition, the transients have very little influence on the position of the ITCZ, in contrast with previous studies that advocated wave–CISK mechanisms (Holton et al. 1971; Lindzen 1974; Hess et al. 1993).

The ITCZ location depends strongly on the convection parameterization. Indeed, even based on the same theoretical considerations, convection schemes yield a variety of ITCZ patterns. In particular, the quasi-equilibrium-based Emanuel (1991) and Betts and Miller (1986) schemes produced, for an equatorial SST maximum, a double ITCZ straddling the equator (Waliser and Somerville 1994) or a single ITCZ at the equator (Frierson 2007), respectively. This dependency on convection parameterization can be found in simple settings as well as in full GCMs. Aquaplanet GCMs switch between a single ITCZ at the equator and a double ITCZ straddling the equator, depending on their convection scheme (Numaguti and Hayashi 1991; Liu et al. 2010; Sumi 1992; Chao 2000; Chao and Chen 2004). The sensitivity of the ITCZ to convection parameterization is also diagnosed in full GCMs, either by changing the convective scheme (Song and Zhang 2009) or by changing parameters of the existing scheme such as lateral entrainment (Terray 1998; Chikira 2010) and reevaporation of precipitation (Bacmeister et al. 2006).

This critical role of convection parameterization is mostly caused by its influence on dynamical feedbacks via the vertical profile of convective heating. The

importance of the vertical heating profile in organizing convection was emphasized in previous studies that showed the influence of secondary processes such as rain reevaporation (Bacmeister et al. 2006), cold top, and downdrafts (Oueslati and Bellon 2013). The vertical profile of diabatic heating was also shown to be crucial to the existence of multiple ITCZ regimes in a simple model (Bellon and Sobel 2010).

Furthermore, convection parameterization influences the ITCZ pattern via the modulation of moisture–convection feedbacks. The interaction between convection and tropospheric humidity is, however, not well represented by GCMs. By and large, GCM cumulus parameterizations are not sufficiently sensitive to free-tropospheric humidity (Derbyshire et al. 2004; Del Genio 2011). This lack of sensitivity results in part from GCMs' tendency to underestimate both the entrainment of environmental air into convective plumes (Kuang and Bretherton 2006) and the reevaporation of rain into the environment (Del Genio 2011).

Additional to its role in the sensitivity of deep convection to free-tropospheric humidity, the lateral entrainment modifies the vertical profiles of both convective heating and moistening by changing the vertical profile of temperature and water vapor in convective plumes. Convective entrainment is therefore a key factor in the convection scheme that modulates convective activity and controls model performances. Recent studies have focused on the convective entrainment, suggesting new parameterizations of this process. Bechtold et al. (2008) proposed an entrainment rate that varies vertically and depends on environmental humidity. Such formulation strengthens the convection sensitivity to environmental moisture. Neale et al. (2008) included more realistic dilution effects through entrainment in the calculation of CAPE. Chikira and Sugiyama (2010) used an entrainment rate proportional to the buoyancy of the convective parcel, thus depending on the surrounding environment. These different studies showed that a better representation of the interaction between cumulus clouds and the surrounding environment allows a significant improvement in the simulation of tropical climatology and variability in GCMs.

To better understand the influence of lateral entrainment on the ITCZ structure, we perform sensitivity experiments using a hierarchy of model configurations (coupled ocean–atmosphere GCM, atmospheric GCM, and aquaplanet GCM), focusing on the relationship between precipitation biases and large-scale circulation systematic errors in a manner similar to Bellucci et al. (2010).

The paper is structured as follows: In section 2, we introduce the models and experiment design. In section 3, we investigate the impact of entrainment on the double

ITCZ bias for the different model configurations. Section 4 presents the sensitivity of large-scale circulation to entrainment changes through a regime sorting analysis. A summary and conclusions are given in section 5.

2. Description of the model and experiments

a. Description of the CNRM-CM5.1

We use the Centre National de Recherches Météorologiques Coupled Global Climate Model, version 5.1 (CNRM-CM5.1), earth system model used for phase 5 of the Coupled Model Intercomparison Project (CMIP5) (Voldoire et al. 2013). It includes version 5.2 of the atmospheric component of the Action de Recherche Petite Echelle Grande Echelle (ARPEGE-Climat) (Déqué et al. 1994). ARPEGE is a spectral model that uses a triangular truncation T127, which corresponds to a horizontal resolution of 1.4° at the equator. The model uses a hybrid sigma pressure vertical coordinate discretized onto 31 vertical levels. The parameterization of radiation combines the longwave radiation scheme Rapid Radiative Transfer Model (RRTM; Mlawer et al. 1997) and a shortwave scheme based on the work of Fouquart and Bonnel (1980). A statistical cloud scheme developed by Ricard and Royer (1993) is included to compute stratiform cloud fraction, stratiform liquid water content, and coefficients of turbulent vertical mixing. Large-scale precipitation is computed from the statistical precipitation scheme described in Smith (1990). Convection is parameterized by a mass-flux scheme where the vertical ascent in the cloud is compensated by a large-scale subsidence. Triggering depends on atmospheric stability and moisture convergence and the closure uses a measure of both cloud-parcel buoyancy and large-scale moisture convergence (Bougeault 1985). The cloud profile is determined by a pseudo moist adiabat incorporating the entrainment of environmental air with a given profile of the entrainment rate ϵ that decreases with altitude, in a manner similar to the one used by Gregory and Rowntree (1990). The entrainment rate is defined as

$$\epsilon = \frac{C}{\min(z, z_{\text{ABL}})}, \quad (1)$$

where C is a constant ($C = 0.185$), z_{ABL} is the atmospheric boundary layer depth, and z is the height above cloud base. The maximum value of the entrainment rate, set at the bottom of the convective column, is about 4.10^{-4} m^{-1} .

The CNRM-CM5.1 includes the land surface scheme Interactions between Soil, Biosphere, and Atmosphere (ISBA) that has been externalized from the atmospheric model through the Surface Externalisée (SURFEX) platform. This interface includes three surface schemes for natural land, inland water (lakes), and sea/ocean areas. The natural land surface scheme is based on the ISBA model (Noilhan and Planton 1989; Noilhan and Mahfouf 1996). Over oceans, the surface fluxes are parameterized using the Exchange Coefficients from Unified Multicampaigns Estimates (ECUME) turbulence scheme (Belamari and Pirani 2007). Over inland water, the exchange coefficients at the air–water interface are computed from the functions of Louis (1979). The oceanic component of CNRM-CM5.1 is the Nucleus for European Modeling of the Ocean (NEMO; version 3.2). The Ocean Atmosphere Sea Ice Soil, version 3 (OASIS3), coupler is used to couple the different components.

b. Hierarchy of model configurations and experiments

To study the impact of convective entrainment on tropical dynamics, we use a hierarchy of model configurations with exactly the same physical parameterizations. This approach is useful to investigate the sensitivity of GCMs to convection parameterization, as it facilitates the identification of robust model behaviors and the dominant processes that respond to parameter changes.

The most realistic model configuration corresponds to the fully coupled ocean–atmosphere CNRM-CM5.1. The coupled model is run over the 21-yr period 1979–99, using the CNRM-CM5.1 historical simulation (HIST) in CMIP5 as initial conditions. The second model configuration corresponds to atmospheric-only experiments commonly referred to as Atmospheric Model Intercomparison Project (AMIP) experiments, using SST prescribed from monthly-mean observations over the 21-yr period 1979–99. The most idealized configuration consists of aquaplanet experiments with idealized SST distributions and perpetual equinoctial solar insolation including the diurnal cycle as presented in Oueslati and Bellon (2013). The SST distribution is specified in a manner similar to the Aqua-Planet Experiment project (Neale and Hoskins 2000). It is zonally symmetric with a maximum of 27°C at the equator,

$$\text{SST}(\phi) = \begin{cases} 27 \left[1 - (1 - k) \sin^2\left(\frac{3\phi}{2}\right) - k \sin^4\left(\frac{3\phi}{2}\right) \right], & \text{if } -\frac{\pi}{3} < \phi < \frac{\pi}{3}, \\ 0, & \text{otherwise,} \end{cases} \quad (2)$$

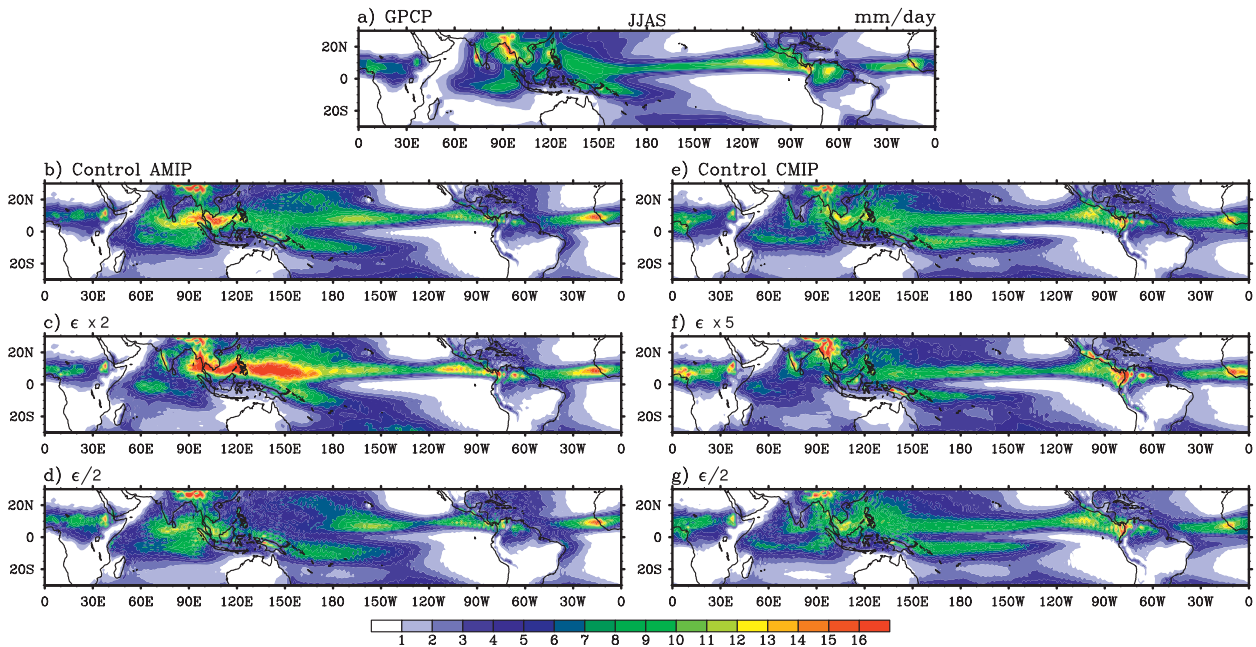


FIG. 1. The 1979–99 mean JJAS precipitation (mm day^{-1}) from (a) GPCP, (b)–(d) AMIP, and (e)–(g) CMIP sensitivity experiments.

where ϕ is the latitude and k is a parameter that controls the tropical SST gradients. Here k is taken equal to 0.4, which corresponds to the threshold for the transition from the double (two maxima of precipitation obtained for weaker off-equatorial SST gradients) to the single (one maximum of precipitation at the equator obtained for larger off-equatorial SST gradients) regime in this model (see Oueslati and Bellon 2013).

Two sensitivity tests were performed with these three model configurations, where the full profile of entrainment is either doubled ($\epsilon \times 2$) or halved ($\epsilon/2$), through doubling or halving the constant C in Eq. (1). To further explore the coupled GCM response, we performed an additional sensitivity experiment where the entrainment rate is multiplied by 5 ($\epsilon \times 5$). In most of the manuscript, we present the CMIP $\epsilon \times 5$ results rather than $\epsilon \times 2$ because the coupled model required a larger entrainment rate than the atmosphere-only model to produce significant differences. Details on this model behavior will be given in section 3.

3. Impact of entrainment on the double ITCZ

Figures 1 and 2 show the precipitation mean for both boreal summer [June–September (JJAS)] and winter [December–March (DJFM)] seasons, respectively, over the period 1979–99 for AMIP ($\epsilon \times 2$ and $\epsilon/2$) and CMIP ($\epsilon \times 5$ and $\epsilon/2$) sensitivity experiments and the corresponding reference simulations (control AMIP and control CMIP). Model results are compared with the

Global Precipitation Climatology Project (GPCP), version 2, dataset (Adler et al. 2003). The JJAS control AMIP run produces the characteristic double ITCZ bias in the tropical Pacific with a zonally oriented southern rainband (see Fig. 1b). This model bias is worse in the coupled model (see Fig. 1e), in response to coupled ocean–atmosphere feedbacks that tend to amplify this bias, favored by warm SST biases in the eastern side of the tropical basins (Lin 2007). This unrealistic zonal extension has been reduced relative to the previous-generation model (CNRM-CM3) mostly as a result of increased horizontal resolution (Voldoire et al. 2013). Figure 1 shows that, in ARPEGE atmosphere-only simulations, the double ITCZ bias affects the central Pacific rather than the eastern Pacific as in other models. It is in fact connected to the simulation of a too zonally elongated SPCZ. Relative to the control AMIP and AMIP $\epsilon/2$ simulations, the AMIP $\epsilon \times 2$ simulation exhibits a considerable weakening of the southern side of the ITCZ (see Figs. 1a,c). In addition, the SPCZ is more confined and its southeast orientation is better represented. Increasing the entrainment results in a reduction of deep convection in the southeastern Pacific and an enhanced precipitation along the ITCZ and the SPCZ (see Fig. 1c). In fact, increasing the entrainment implies more lateral mixing between cumulus clouds and the environmental dry air, favoring the dilution of convective plumes and the inhibition of deep convection. The enhanced lateral mixing results in more turbulent fluxes and a deeper ABL in subsidence regions (see Fig. 3,

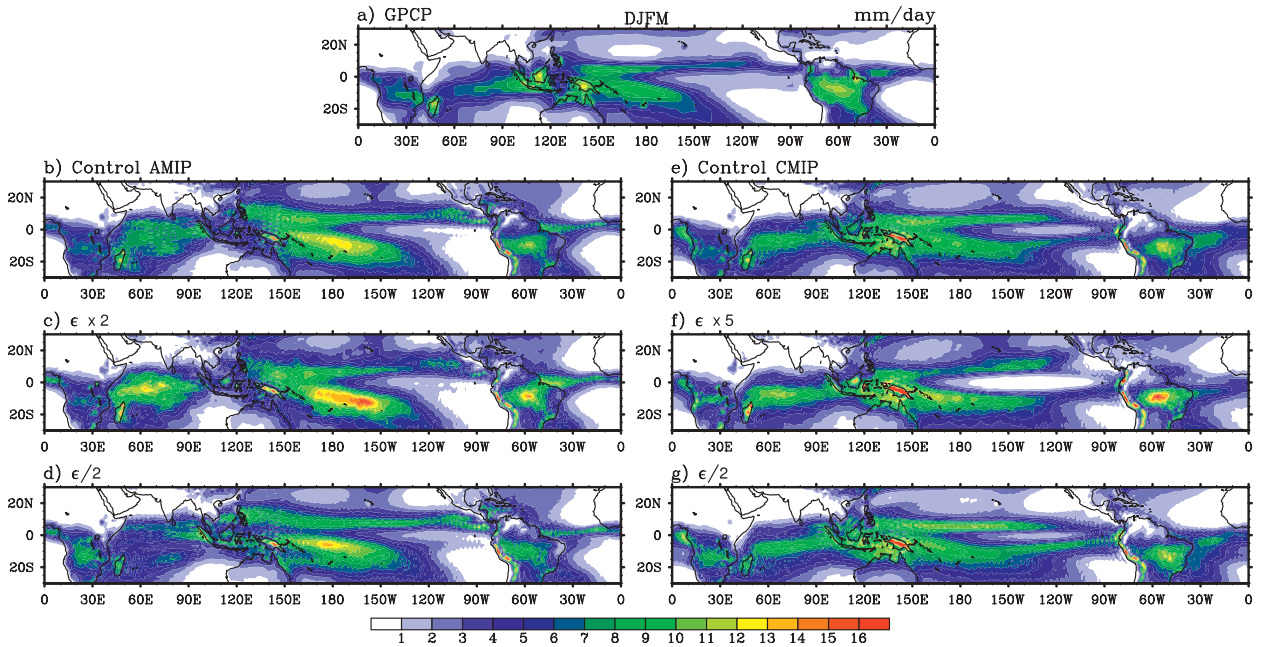


FIG. 2. The 1979–99 mean DJFM precipitation (mm day^{-1}) from (a) GPCP, (b)–(d) AMIP, and (e)–(g) CMIP sensitivity experiments.

AMIP). This deeper ABL is advected toward the deep convective regions (ITCZ and SPCZ), and it acts as an additional supply of moisture that intensifies deep convection in these regions. As a result, deep convection tends to be stronger because increased entrainment strengthens the free-tropospheric humidity–convection feedback. This intensified convective activity is consistent with the GPCP observations in the central and eastern Pacific; however, it leads to an overestimation of precipitation over the west Pacific warm pool in association with a stronger Walker circulation (diagnosed by the velocity potential of the wind at 200 hPa; not shown) and a stronger Asian monsoon. A similar behavior of the tropical convection has been noticed in Song and Zhang (2009) when using the Community Climate System

Model, version 3.0 (CCSM3.0). Their atmospheric model simulation with a revised scheme (with a new closure) shows a considerable reduction of the double ITCZ but also more precipitation in the western Pacific, as a result of a stronger positive circulation–convection feedback. The coupled simulations show the same sensitivity to a change in entrainment, with a less pronounced double ITCZ bias simulated by the $\epsilon \times 5$ experiment (see Figs. 1f,g). However, precipitation distribution in the southern Pacific is still poorly simulated, relative to the atmosphere-only simulations, because of coupled ocean–atmosphere feedbacks that amplify the double ITCZ bias (Lin 2007) and counteract the improvement from enhanced lateral entrainment. The overestimation of precipitation shown in the AMIP $\epsilon \times 2$ simulation is not

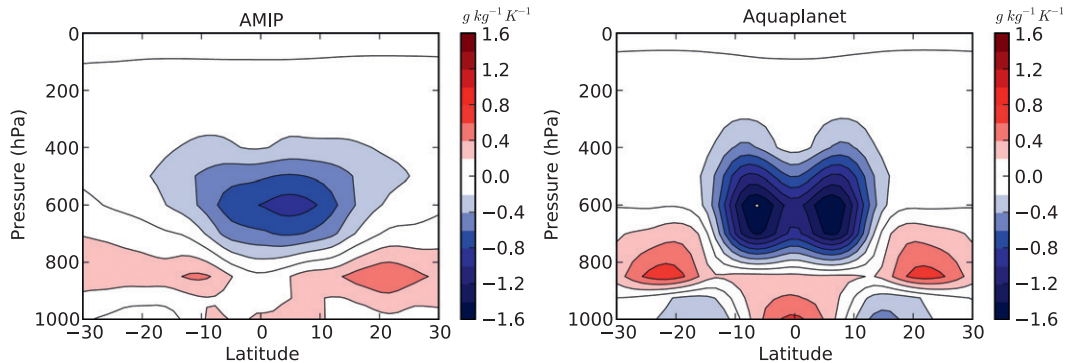


FIG. 3. Difference in zonal-mean specific humidity between $\epsilon \times 2$ and $\epsilon/2$ of (left) AMIP and (right) aquaplanet experiments in the tropics. Negative (positive) values on the x axis indicate southern (northern) latitudes.

observed in the $\epsilon \times 5$ CMIP simulation because of the SST response to increased cloudiness.

The DJFM AMIP simulations do not really suffer from the double ITCZ bias (see Figs. 2a,b). However, the sensitivity of ITCZ to entrainment change is clearly noticed when comparing the AMIP $\epsilon/2$ and $\epsilon \times 2$ experiments, with no more southern ITCZ in the AMIP $\epsilon \times 2$ simulation. The DJFM CMIP simulations show the same sensitivity to entrainment change, with a reduction of the zonal extension of the southern side of the ITCZ in the $\epsilon \times 5$ experiment (see Figs. 2f,g). However, in both the AMIP and CMIP simulations, the SPCZ is unrealistically strengthened and Indian Ocean precipitation is overestimated, for the reasons mentioned above.

The sensitivity to entrainment experiments shows that alleviating the double ITCZ bias in the AMIP simulation (see Figs. 1c, 2c) is not sufficient to significantly reduce the double ITCZ bias in the coupled model (see Figs. 1e, 2e). This contrast between AMIP and CMIP responses to enhanced entrainment results from the fact that the coupled ocean–atmosphere feedbacks control most of the amplitude of the double ITCZ bias in the coupled model: the improvement obtained by changing a parameter in AMIP experiment can be significantly reduced by coupled feedbacks in the corresponding CMIP experiment.

Figures 4 and 5 show the seasonal cycle of monthly precipitation averaged over two longitudinal sectors of the Pacific Ocean from GPCP, AMIP, and CMIP runs, in a manner similar to Dai (2006). In the eastern Pacific (80°–120°W), the observations show the dominance of the northern ITCZ from May to December and the double ITCZ structure in March and April (see Fig. 4a). Relative to the control AMIP and AMIP $\epsilon/2$ experiment, the AMIP $\epsilon \times 2$ experiment is in better agreement with GPCP data (see Figs. 4a–d). In particular, the AMIP $\epsilon \times 2$ experiment reproduces the intensification of precipitation rates in boreal summer (JJA) and simulates a weaker southern side of the ITCZ. However, because of the dilution effect of entrainment, the double ITCZ structure observed in boreal spring (MA) is largely underestimated in the AMIP $\epsilon \times 2$ experiment. In contrast, the AMIP $\epsilon/2$ experiment simulates a strong southern ITCZ that persists until June and, like the control AMIP, exhibits the same precipitation intensity all year round north of the equator. We clearly see that, unlike the control CMIP and CMIP $\epsilon/2$ experiments, which simulate a single ITCZ that moves across the equator following the solar forcing, the CMIP $\epsilon \times 5$ experiment simulates a more realistic seasonal cycle with a weaker southern ITCZ (see Figs. 4e–g). However, because of the strong inhibition of convection by entrainment, no more northern ITCZ is simulated in January and February (see Fig. 4f). In the northeastern Pacific, during this particular

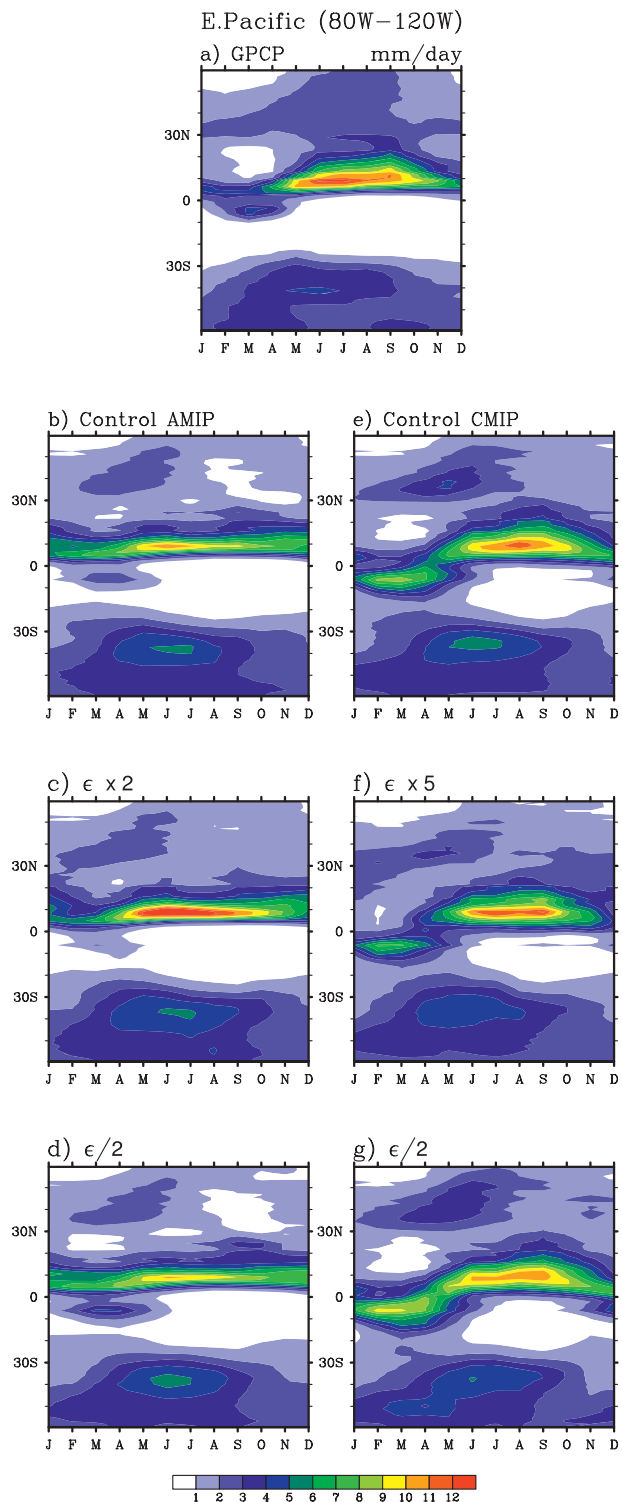


FIG. 4. Seasonal cycle of precipitation in the eastern Pacific (80°–120°W) for (a) GPCP, (b)–(d) AMIP, and (e)–(g) CMIP sensitivity experiments.

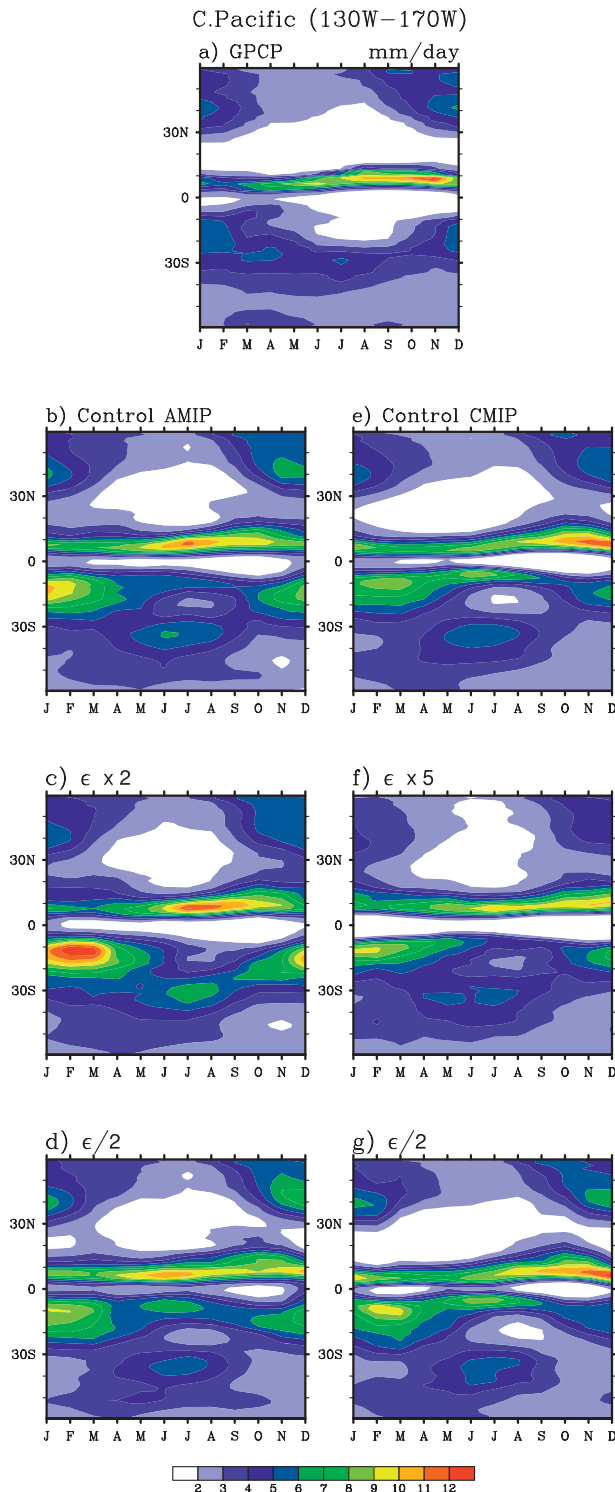


FIG. 5. Seasonal cycle of precipitation in the central Pacific (130°–170°W) for (a) GPCP, (b)–(d) AMIP, and (e)–(g) CMIP sensitivity experiments.

season, coupled feedbacks have a negative feedback on convection (see Fig. 2) that is further enhanced by the diluting effect of entrainment.

Over the central Pacific (130°–170°W), both the control AMIP and control CMIP produce a persistent double ITCZ error with a southern rain belt present throughout the year (see Figs. 5b,e). This bias is enhanced in $\epsilon/2$ experiments. In contrast, the seasonal cycle of the ITCZ is improved in the AMIP $\epsilon \times 2$ experiment with the disappearance of the southern rain belt in boreal summer (see Fig. 5c). However, it still persists too long relative to observations. The CMIP $\epsilon \times 5$ experiment shows the same sensitivity to entrainment as the atmosphere-only run, but with a smaller improvement of the seasonal cycle of precipitation (see Fig. 5f). The unrealistic strengthened SPCZ, shown in Fig. 2c appears in the seasonal cycle with overestimated southern precipitation in boreal winter. As already mentioned, deep convection tends to be stronger, because of strengthened free-tropospheric humidity–convection feedback in response to increased entrainment.

To compare with the aquaplanet configuration, we plot in Fig. 6 the zonal-mean precipitation from GPCP data, the AMIP and CMIP runs, averaged over central and eastern Pacific (80°–170°W; see Figs. 6a,b), and from aquaplanet runs (see Fig. 6c). For CMIP simulations, we show both the $\epsilon \times 2$ and the $\epsilon \times 5$ experiments. For increasing entrainment rates, both the AMIP and aquaplanet configurations show a transition from a double ITCZ structure, with two off-equatorial precipitation peaks, to a single ITCZ structure, with one maximum of precipitation located at the equator in the aquaplanet run and near 10°N in the AMIP run. The CMIP zonal-mean precipitation exhibits the same sensitivity to lateral entrainment as in AMIP simulations. However, in response to doubled entrainment rate, the coupled simulation yields a less pronounced weakening of the southern side of the ITCZ relative to the AMIP simulation. For the $\epsilon \times 5$ experiment, we clearly see that the single ITCZ structure is better represented relative to $\epsilon \times 2$, suggesting again that, in the coupled GCM, convection inhibition through entrainment needs to be stronger to overcome the impact of ocean–atmosphere feedbacks.

The sensitivity of the ITCZ structure to entrainment is robust across the three model configurations. This suggests that it is controlled by physical atmospheric processes independent, at first order, of land surface effects, even though coupled ocean–atmosphere processes do modulate this sensitivity significantly. The results also suggest that a better representation of entrainment is a key factor for more realistic precipitation distributions. Indeed, this study shows that alleviating the double ITCZ bias in the AMIP simulations is not sufficient to reduce

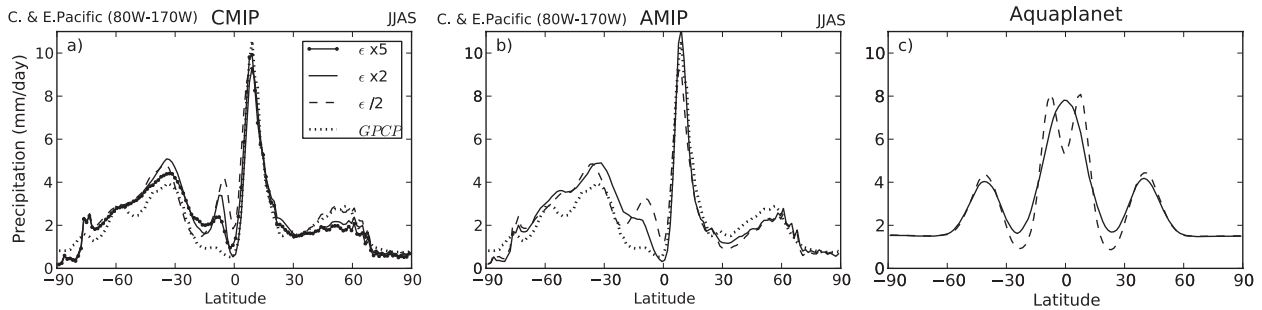


FIG. 6. Zonal-mean precipitation from (a) GPCP data and CMIP, (b) AMIP, and (c) aquaplanet sensitivity experiments. Negative (positive) values on the x axis indicate southern (northern) latitudes.

the double ITCZ bias in the coupled mode. A good representation of coupled feedbacks is also essential to eradicate the double ITCZ bias in coupled models. In addition, including some other processes unfavorable for deep convection (e.g., convective downdrafts; Oueslati and Bellon 2013) might have to be considered. Increasing the convective entrainment also causes an overestimation of precipitation in the center of convergence zones. This might be compensated for by tuning parameters that tend to reduce convection uniformly (such as the coefficient in the Kuo closure in ARPEGE-Climat).

4. Impact of entrainment on the tropical circulation

a. Diagnosing the tropical circulation change by a regime-sorting analysis

Changes in precipitation distribution in response to lateral entrainment change (shown in section 3) strongly depend on the large-scale atmospheric circulation. To analyze the differences in tropical circulation between the two sensitivity tests, we adopt the sorting methodology proposed by Bony et al. (2004) where the monthly-mean midtropospheric (500 hPa) vertical pressure velocity ω is used as a proxy for large-scale ascent ($\omega_{500} < 0$) or subsidence ($\omega_{500} > 0$). The columns of the tropical atmosphere (30°S – 30°N) are sorted into 5-hPa bins of ω_{500} . The resulting probability distribution

functions (PDF) of ω_{500} are shown in Fig. 7 for the 40-yr European Centre for Medium-Range Weather Forecasts (ECMWF) Re-Analysis (ERA-40) and for the CMIP, AMIP, and aquaplanet simulations. The reanalysis PDF shows that regimes of large-scale subsidence are the most frequent in the tropics, constrained by the clear-sky radiative cooling. The $\epsilon/2$ experiments fail in simulating this dominance of subsidence regimes. Instead, it produces an unrealistic bimodal structure of the PDF with the same frequency of subsiding and ascending events. In contrast, AMIP $\epsilon \times 2$ and CMIP $\epsilon \times 5$ provide a PDF in agreement with observations, with enhanced frequency of weak-to-moderate subsiding regimes ($0 \text{ hPa day}^{-1} < \omega_{500} < 30 \text{ hPa day}^{-1}$) and reduced frequency of weak-to-moderate ascending regimes ($-60 \text{ hPa day}^{-1} < \omega_{500} < 0 \text{ hPa day}^{-1}$). However, the occurrence of subsidence is still underestimated relative to the reanalysis. The lower frequency of moderate ascending regimes in the $\epsilon \times 2$ and $\epsilon \times 5$ experiments is explained by the inhibition of convection in response to enhanced lateral entrainment. This inhibition allows the development of more intense shallow convection associated with increased turbulent fluxes and a deeper ABL in subsidence regions (see Fig. 3). This deeper ABL favors moisture convergence into the deep convective regions (ITCZ and SPCZ), thereby increasing precipitation. The control on the tropospheric moisture supply to the

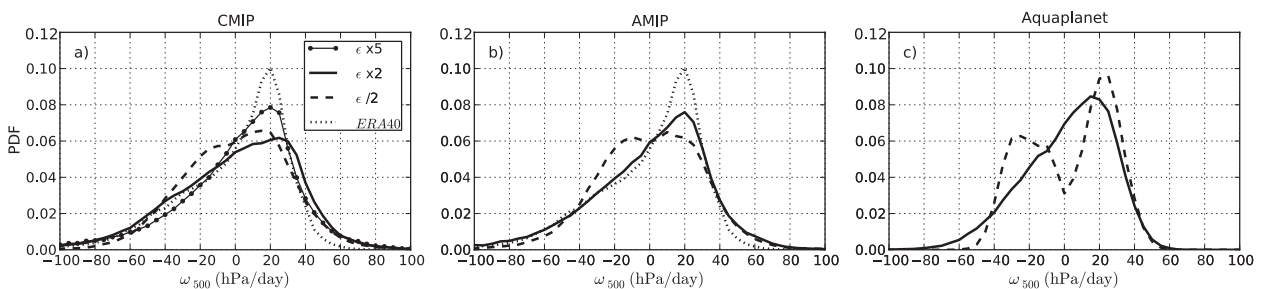


FIG. 7. PDF of the 500-hPa large-scale vertical velocity ω_{500} in the tropics (30°S – 30°N) derived from (a) observations (ERA-40) and CMIP, (b) AMIP, and (c) aquaplanet sensitivity experiments.

convergence zones by the shallow convection has already been emphasized by Neggers et al. (2007) and termed the shallow cumulus humidity throttle mechanism. The intensified convective activity in ascending regions explains the enhanced frequency of strong convective regimes ($\omega_{500} < -60$ hPa day⁻¹) and the larger precipitation rates produced by $\epsilon \times 2$ and $\epsilon \times 5$ in the center of convergence zones (see Figs. 1, 2, 6).

The sensitivity of the tropical circulation to lateral entrainment observed in AMIP and CMIP simulations is clearly reproduced by the aquaplanet model, showing the robustness of the associated atmospheric mechanisms. The bimodality of the PDF in the $\epsilon/2$ experiments is even more pronounced, suggesting that aquaplanets can be a useful test bed to study the model sensitivity to parameter changes.

b. Mechanisms responsible for the tropical circulation change

1) UNDERSTANDING THE PDF SHAPE THROUGH THE ENERGY BUDGET

To isolate the mechanisms responsible for the tropical circulation change between the two sensitivity tests and to understand the processes behind the transition from the bimodal to the unimodal PDF, we consider the vertically integrated budget of dry static energy at equilibrium,

$$\left\langle \frac{\partial s}{\partial t} \right\rangle = 0 = - \left\langle \omega \frac{\partial s}{\partial p} \right\rangle - \langle \mathbf{v} \cdot \nabla s \rangle + Q_{\text{cond}} + Q_{\text{rad}} + Q_{\text{tur}}, \quad (3)$$

where s is the dry static energy ($s = c_p T + gz$, where c_p is the specific heat at constant pressure, T is the temperature, g is the gravitational acceleration, and z is altitude), ω is the vertical speed, p is pressure, and \mathbf{v} is the horizontal velocity. The angle brackets represent the mass-weighted vertical integral from the surface to the top of the atmosphere and are defined, for a quantity A , as the expression; $\langle A \rangle = \int_0^{p_s} A(dp/g) Q_{\text{cond}} = LP$ is the column-integrated condensation, where P is the total surface precipitation and L is the latent heat of condensation; Q_{rad} is the column-integrated radiative cooling; and Q_{tur} is the surface sensible heat flux.

The vertical advection of s may be expressed as

$$\left\langle \omega \frac{\partial s}{\partial p} \right\rangle = - \langle \mathbf{v} \cdot \nabla s \rangle + Q_{\text{cond}} + Q_{\text{rad}} + Q_{\text{tur}}. \quad (4)$$

If we divide Eq. (4) by the vertically integrated gradient of dry static energy over the troposphere

$$\left\langle \frac{\partial s}{\partial p} \right\rangle_{\text{Tropo}} = \int_{p_t}^{p_s} \frac{\partial s}{\partial p} \frac{dp}{g} = \frac{s_s - s_t}{g},$$

where p_s is the surface pressure, p_t is the pressure at the tropopause, s_s is the dry static energy at the surface, and s_t is the dry static energy at the tropopause, we can express a vertical speed characteristic of energy advection ω^s as the sum of four contributions from advection, condensation, radiation, and turbulence,

$$\omega^s = \omega_{\text{advH}}^s + \omega_{\text{cond}}^s + \omega_{\text{rad}}^s + \omega_{\text{tur}}^s, \quad (5)$$

with

$$\begin{aligned} \omega^s &= \frac{\left\langle \omega \frac{\partial s}{\partial p} \right\rangle}{\left\langle \frac{\partial s}{\partial p} \right\rangle_{\text{Tropo}}}, \\ \omega_{\text{advH}}^s &= \frac{- \langle \mathbf{v} \cdot \nabla s \rangle}{\left\langle \frac{\partial s}{\partial p} \right\rangle_{\text{Tropo}}}, \\ \omega_{\text{cond}}^s &= \frac{Q_{\text{cond}}}{\left\langle \frac{\partial s}{\partial p} \right\rangle_{\text{Tropo}}}, \\ \omega_{\text{rad}}^s &= \frac{Q_{\text{rad}}}{\left\langle \frac{\partial s}{\partial p} \right\rangle_{\text{Tropo}}}, \quad \text{and} \\ \omega_{\text{tur}}^s &= \frac{Q_{\text{tur}}}{\left\langle \frac{\partial s}{\partial p} \right\rangle_{\text{Tropo}}}. \end{aligned}$$

The vertical velocity ω^s is representative of the large-scale vertical motion of the atmosphere and is therefore comparable to ω_{500} . We compute the PDF of ω^s for both aquaplanet and AMIP simulations, following the same method as for ω_{500} . These PDFs are shown in Fig. 8. The PDFs of ω^s have the same properties as those of ω_{500} , with a bimodal PDF in $\epsilon/2$ and a unimodal PDF in $\epsilon \times 2$, although a hint of bimodality can be seen in the ω^s PDF of the $\epsilon \times 2$ aquaplanet simulation. Similarly to ω_{500} , the PDF of ω^s shows the decreased occurrence of moderate ascending regimes and the increased occurrence of subsidence regimes in response to quadrupled lateral entrainment.

To investigate the mechanisms that control the shape of the PDF (i.e., the bimodal or the unimodal structure), we consider Eq. (5) and compute the PDFs of the different contributions to ω^s for the two sensitivity experiments. The PDFs of ω_{advH}^s , ω_{cond}^s , ω_{rad}^s , and ω_{tur}^s are presented in Fig. 9. Both in the AMIP and aquaplanet configurations, these PDFs exhibit the same

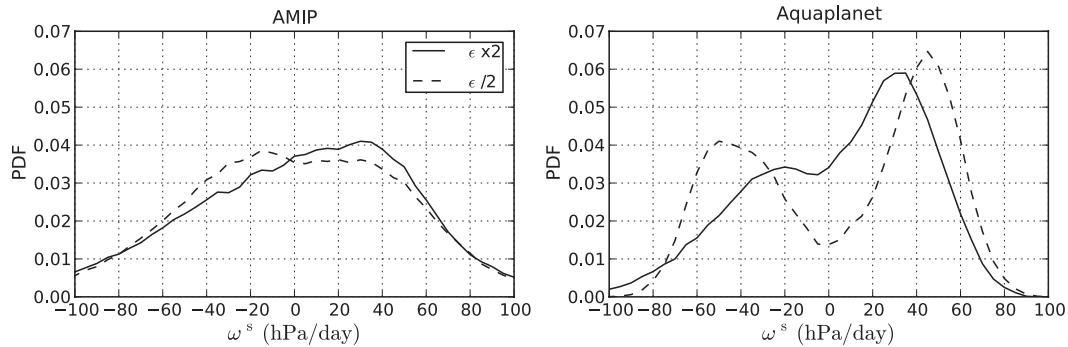


FIG. 8. PDF of ω^s in the tropics (30°S – 30°N) derived from (left) AMIP and (right) aquaplanet sensitivity experiments.

characteristics. Indeed, the PDF of the sum is not directly related to the PDFs of each term of the sum. However, if a PDF of one term is a Dirac delta function, that term has no influence on the PDF of the sum. On the other hand, if the PDF of one term has large spread, the PDF of the sum will at least exhibit as large a spread. If one term has a bimodal PDF, the bimodality will be conserved in the PDF of the sum, if the PDFs of the other terms exhibit a small spread. Figure 9 shows that only the contribution from condensation is bimodal. All the other contributions are unimodal, and their spreads are small relative to those of ω^s and ω_{cond}^s . Therefore, the bimodality of ω^s results most likely from the bimodality of ω_{cond}^s and the transition from unimodality to bimodality results from feedbacks between precipitation and vertical dynamics. Condensation controls the atmospheric vertical motion by modulating temperature and geopotential gradients through latent heat release inside cumulus clouds and inducing low-level convergence and upward motion. Large-scale low-level convergence, in turn, supplies moisture to the atmospheric column that further drives precipitation. Changing the convective entrainment modifies this interaction between large-scale circulation and precipitation.

Increasing the entrainment increases the sensitivity of deep convection to the surrounding environment and in particular to free-tropospheric humidity, thereby strengthening its sensitivity to large-scale transport of humidity and in particular to humidity convergence. Figure 9 shows some changes in the radiative contribution between the two experiments. This suggests that cloud feedbacks contribute to the tropical circulation change and thus to the ITCZ structure. In particular, convective clouds cause a significant radiative warming that adds to the latent heating and enhance the dynamical response.

Our energetic analysis of the different contributions to the ω^s PDF highlights the importance of the interaction between large-scale circulation and precipitation in controlling the bimodality or the unimodality of the PDF. The same analysis was carried out over the double ITCZ (DI) region (20°S – 0° , 100° – 150°W ; Bellucci et al. 2010). It shows that the regional PDF in the DI region and the global PDF in the tropics have similar behaviors. The change in the feedbacks between precipitation and dynamics cause the change in the PDF of ω_{500} , both regionally and globally, controlling therefore the precipitation biases and particularly the presence and the amplitude of the double ITCZ bias.

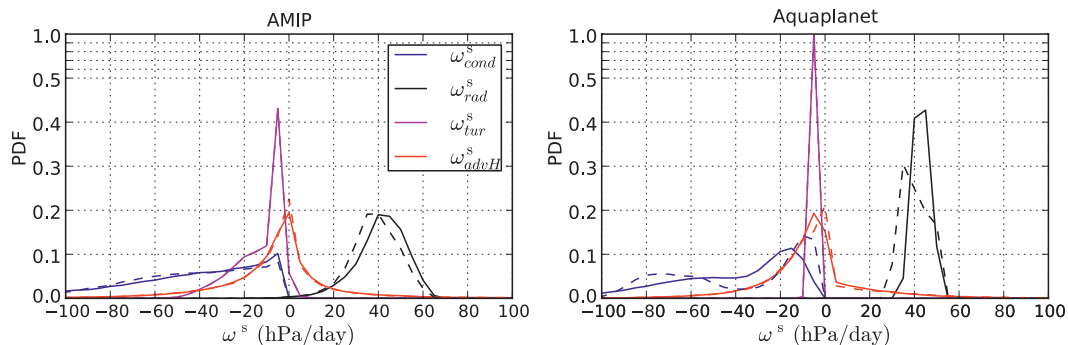


FIG. 9. PDF of the different contributions to ω^s in the tropics (30°S – 30°N) derived from the two sensitivity experiments, $\epsilon \times 2$ (solid) and $\epsilon/2$ (dashed), for both (left) AMIP and (right) aquaplanet sensitivity experiments.

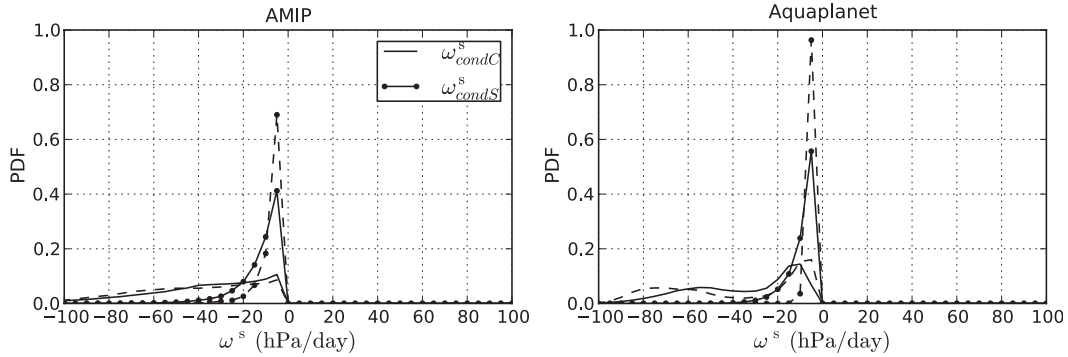


FIG. 10. PDF of convective ω^s_{condC} and stratiform ω^s_{condS} contributions to condensation in the tropics (30°S–30°N) derived from the two sensitivity experiments, $\epsilon \times 2$ (solid) and $\epsilon/2$ (dashed), for both (left) AMIP and (right) aquaplanet sensitivity experiments.

The contribution to ω^s from condensation can be partitioned into two contributions, one from the deep-convection scheme ω^s_{condC} and the other from the large-scale stratiform scheme ω^s_{condS} , with

$$\omega^s_{\text{condC}} = \frac{LP_C}{\left\langle \frac{\partial s}{\partial p} \right\rangle_{\text{Tropo}}}$$

and

$$\omega^s_{\text{condS}} = \frac{LP_S}{\left\langle \frac{\partial s}{\partial p} \right\rangle_{\text{Tropo}}},$$

where P_C is the convective precipitation and P_S is the large-scale precipitation. The PDFs of ω^s_{condC} and ω^s_{condS} are shown in Fig. 10.

In both the AMIP and aquaplanet configurations, only the convective contribution is bimodal. The stratiform contribution is unimodal, and its spread is smaller than

that of ω^s_{condC} . Therefore, the bimodality of ω^s_{cond} results from the bimodality of ω^s_{condC} and the atmospheric circulation is driven by deep cumulus convection rather than by large-scale condensation. The mechanism at play is similar to that in CISK. Decreasing the entrainment increases the convective latent heating for a given thermodynamic environment and thereby the response of the circulation. The model behaves then more and more as in the CISK theory. The double ITCZ bias is therefore associated with an active CISK mechanism in the GCM.

2) RELATIONSHIP BETWEEN PRECIPITATION AND LARGE-SCALE CIRCULATION

The energy budget analysis presented in section 4b(1) emphasized the link between large-scale vertical motion and convective activity. To further explore this dynamical link, we compute the average precipitation for each ω_{500} regime in the observations and in the GCM simulations, as well as the average convective and stratiform contributions in the GCM simulations (see Fig. 11).

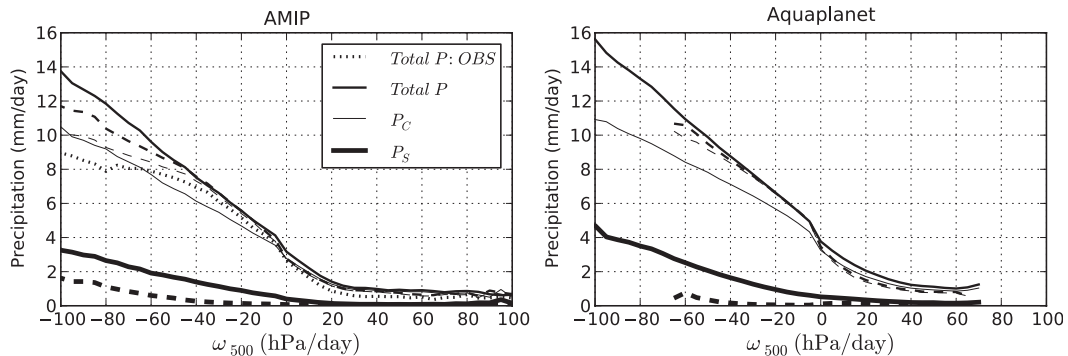


FIG. 11. Precipitation in each dynamical regime of the tropics (30°S–30°N) derived from observations (dotted) and the two sensitivity experiments, $\epsilon \times 2$ (solid) and $\epsilon/2$ (dashed), for both (left) AMIP and (right) aquaplanet sensitivity experiments.

Both in AMIP and aquaplanet configurations, the regime-sorted precipitation exhibits the same characteristics. The interaction between convection and circulation appears in the regime-sorted diagram, with the largest precipitation intensities occurring in ascending regions ($\omega_{500} < 0$) and the weaker precipitation intensities occurring in subsiding regions ($\omega_{500} > 0$), as expected. The difference between the two sensitivity simulations $\epsilon \times 2$ and $\epsilon/2$ in regime-sorted total precipitation only appears for strong ascending motion ($\omega_{500} < -60$ hPa day⁻¹). In these dynamical regimes, total precipitation in $\epsilon \times 2$ is larger than that in $\epsilon/2$, which together with the increased frequency of these particular regimes is consistent with the larger precipitation produced by the $\epsilon \times 2$ experiment along the ITCZ and SPCZ (see Figs. 1c, 2c). Relative to the observations, the two simulations overestimate total precipitation in all the vertical circulation regimes. The largest model–observation errors are observed for strong ascending regimes. The difference in the occurrence of weak-to-moderate ascending regimes between the two sensitivity experiments is associated with a smaller convective precipitation rate produced in $\epsilon \times 2$ within these regimes (see Fig. 11). The decrease in convective precipitation in $\epsilon \times 2$ is compensated by an increase of large-scale precipitation. In particular, the larger precipitation produced by $\epsilon \times 2$ within strong ascending regimes is explained by the increased stratiform precipitation rate, which is expected to result from the uplift of a more abundant ABL moisture from cumulus convection inhibition.

Partitioning between convective and large-scale precipitation in the tropics can be measured by a convective-to-total precipitation (P_c/P) ratio (Dai 2006). This ratio is more realistic in $\epsilon \times 2$, as about 80% of the total precipitation comes from convection (excluding the subtropical dry areas), compared with 95% in $\epsilon/2$. However, the P_c/P ratio is still larger than the observed 45%–65% one, estimated by the Tropical Rainfall Measuring Mission (TRMM) satellite observations (Dai 2006). Although the P_c/P ratio is not fully comparable between the models and the TRMM observations, it gives a qualitative measure of the contribution of both convective and stratiform components to the total precipitation. The same ratio was calculated for the coupled simulations. Ratios of 60%–70% and 85% of the total precipitation were obtained in $\epsilon \times 5$ and $\epsilon \times 2$, respectively, in contrast to 95% obtained in the coupled $\epsilon/2$ experiment. The biases in the convective versus stratiform precipitation ratio have already been diagnosed in most current coupled GCMs (CGCMs; Dai 2006). A better parameterization of the lateral entrainment seems to also reduce this bias.

The overestimation of rainfall by models for a given vertical regime shown in Fig. 11 has already been identified in the DI region by Bellucci et al. (2010). However, according to their study, this error in the magnitude of precipitation plays a minor role in the double ITCZ bias relative to the error in the frequency of occurrence of dynamical regimes. This conclusion is also verified in the present work by computing the ω_{500} PDF and the average precipitation for each ω_{500} regime in the DI region for AMIP simulations (see Fig. 12). In fact, the $\epsilon \times 2$ and $\epsilon/2$ experiments simulate similar precipitation rates within strong ascending regimes in the double ITCZ region, while the double ITCZ problem is considerably alleviated in the $\epsilon \times 2$ experiment (see Fig. 12b). The rainfall intensity in strong ascending regimes plays a smaller role in the double ITCZ bias because of the lower frequency of these particular regimes in the double ITCZ region (see Fig. 12a). In addition, it can be shown using a metric of the double ITCZ bias that more than 90% of the difference between the $\epsilon \times 2$ and $\epsilon/2$ experiments is caused by the change in the PDF of ω_{500} . The sensitivity of precipitation and large-scale circulation to lateral entrainment at the regional scale (in the DI region) is thus similar to that at the global scale (in the tropics). The largest differences in regime frequency between the two experiments in the DI region are observed for weak-to-moderate ascending regimes and weak subsiding regimes (see Fig. 12a), similar to the global-scale differences (see Fig. 7), pointing out the importance of these regimes in the double ITCZ bias.

A more quantitative estimate of the contribution of each vertical regime to the total tropical precipitation was proposed by Bellucci et al. (2010), in which the regime-sorted precipitation is weighted by the corresponding ω_{500} PDF. The obtained distributions are shown in Fig. 13. In both the AMIP and aquaplanet configurations, the weighted precipitation exhibits the same characteristics, although, unlike the AMIP simulation, a bimodal structure is present in the $\epsilon/2$ aquaplanet distribution, because of the strong bimodality of the corresponding PDF (see Fig. 7). The largest contribution to precipitation in the tropics derives from weak-to-moderate ascending regimes, with a maximum for ω_{500} in the from -40 to -20 hPa day⁻¹ range. The two sensitivity experiments do capture a maximum contribution in this range, but the maximum is overestimated because of the overestimated frequency of these regimes relative to the observations. In contrast to $\epsilon/2$, $\epsilon \times 2$ presents a more realistic distribution associated with a more realistic PDF that is particularly explained by a decreased frequency of moderate ascending regimes. However, $\epsilon \times 2$ overestimates the contribution of strong ascending regimes to precipitation; this is because of the

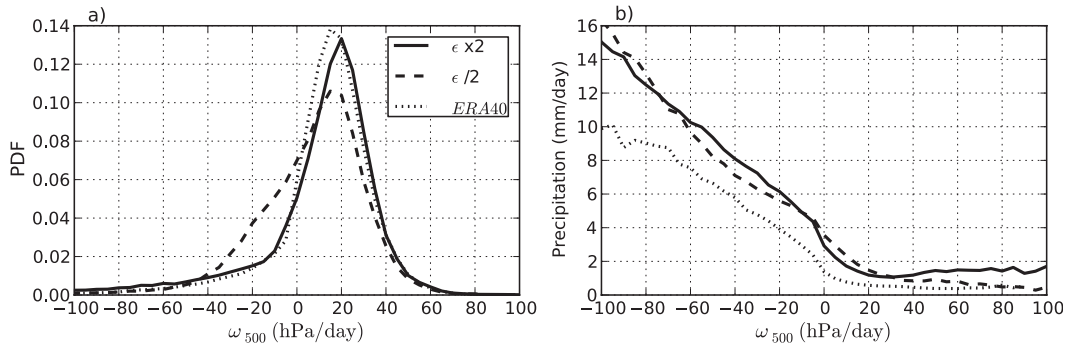


FIG. 12. (a) PDF of the 500-hPa large-scale vertical velocity ω_{500} and (b) precipitation in each dynamical regime over the double ITCZ region (20°S–0°, 100°–150°W) derived from observations and AMIP sensitivity experiments.

overestimation of both the frequency of occurrence of vertical regimes and the associated precipitation. As already mentioned, this error has a minor role in the double ITCZ problem.

In summary, the double ITCZ bias appears to be associated with errors in the frequency of occurrence of dynamical regimes, and in particular that of weak-to-moderate ascending regimes, since $\epsilon \times 2$ and $\epsilon / 2$ simulate similar precipitation rates in these regimes (see Fig. 11). The emergence of a bimodal ω_{500} PDF is associated with an even stronger double ITCZ. This result contradicts the explanation provided by Chikira (2010) of the weakening of the southern side of the ITCZ in response to a new formulation of entrainment rate that varies vertically depending on the surrounding environment. That study argues that deep convection in the southeastern Pacific is suppressed by the additional drying of the lower troposphere that is produced by the replacement of the moist effect of shallow convection by the drying effect of relatively deeper convection associated with cumulus congestus clouds. Bellucci et al. (2010) stated that the error in the frequency of occurrence of deep convection in the southeastern Pacific is caused by ocean–atmosphere

interactions. However, our atmosphere-only experiments (in particular with $\epsilon / 2$) show that atmospheric processes can account for some of this bias.

5. Summary and conclusions

This study investigates the impact of lateral entrainment in convective plumes on the double ITCZ systematic bias affecting state-of-the-art coupled general circulation models. Sensitivity studies to the entrainment parameter are performed in a hierarchy of models (coupled ocean–atmosphere GCM, atmospheric GCM, and aquaplanet GCM). The change in ITCZ structure is examined in relation with the representation of the tropical circulation, using a regime-sorting approach applied to the midtropospheric vertical wind ω_{500} .

Results show that the sensitivity of the ITCZ structure to lateral entrainment is robust across the three model configurations. In response to an increased entrainment rate, the double ITCZ problem is considerably reduced. Increasing the entrainment eases the dilution of convective plumes and the inhibition of deep convection to the benefit of a more intense shallow convection,

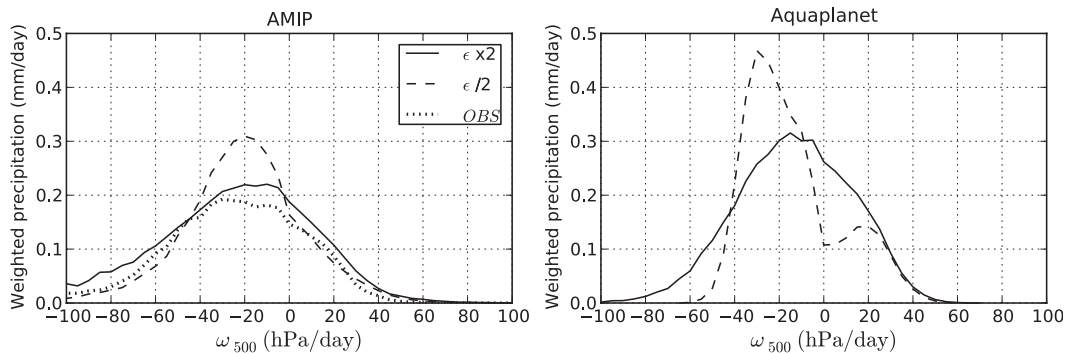


FIG. 13. Precipitation in each dynamical regime of the tropics (30°S–30°N) weighted by the PDF of ω_{500} , derived from (left) observations and AMIP and (right) aquaplanet sensitivity experiments.

associated with increased turbulent fluxes and a deeper ABL. The dilution effect of entrainment reduces considerably the precipitation over subsidence regions and in particular over the southeastern Pacific. As entrainment increases, deep convection becomes more sensitive to free-tropospheric humidity and moisture–convection feedbacks become stronger, resulting in stronger precipitation along the ITCZ. The southeast orientation and the zonal extent of the SPCZ are better simulated in boreal summer. These improvements are obtained at the expense of precipitation in the center of convergence zones that is overestimated, especially in AMIP simulations (e.g., South Asian and western Pacific monsoons, austral summer SPCZ). The overestimation of precipitation over these regions is associated with a strengthened Walker circulation. Similar results were obtained in Terray (1998) in response to entrainment change. In his study, the stronger circulation was pointed out as a cause of the reduction of the double ITCZ bias. However, in our study, the circulation seems to change in nature as the PDF of ω_{500} shows, through convection–circulation feedbacks. In addition, in our study, only the Walker circulation is strengthened. The Hadley circulation is actually weakened. The reasons behind this behavior need to be further investigated. Indeed, this behavior is consistent with the study of Oort and Yienger (1996) where it is shown that the strength of the Hadley cells are strongly and inversely correlated with the anomalies of the strength of the Walker circulation.

Attempts to link precipitation and large-scale circulation systematic errors revealed that the double ITCZ bias is associated with a bimodal PDF of ω_{500} because of an erroneous high frequency of moderate ascending regimes and a lower frequency of shallow convective regimes. This result contradicts the results of Chikira (2010) where the suppression of deep convection in the southeastern Pacific is attributed to the additional drying of the lower troposphere that is produced by the replacement of the moist effect of shallow convection by the drying effect of relatively deeper convection associated with cumulus congestus clouds. Also, our AMIP experiments show that errors in the frequency of occurrence of vertical regimes can result from atmospheric mechanisms only, contrary to Bellucci et al. (2010), who attributed the errors to ocean–atmosphere interactions.

Mechanisms responsible for the tropical circulation changes are examined by analyzing the vertically integrated budget of dry static energy. This energetic analysis highlights the importance of the interaction between large-scale circulation and moist cumulus convection in controlling the bimodality or the unimodality of the ω_{500} PDF and therefore the presence and the amplitude of the double ITCZ bias. Examination of

the regime-sorted precipitation shows that the double ITCZ is associated with errors in the frequency of occurrence of vertical regimes, as concluded by Bellucci et al. (2010), rather than the error in precipitation intensity within each regime. The error in the frequency of vertical regimes is associated with cumulus convection, while the error in precipitation intensity is associated with large-scale condensation. In our sensitivity experiments, increasing the lateral entrainment rate improves the simulation of the frequency of vertical regimes, in particular that of weak-to-moderate ascending regimes. Such an improvement seems to be instrumental to alleviate the double ITCZ bias. Because of the dilution effect of entrainment, the SST threshold leading to the onset of convection in the southeastern Pacific is more restrictive, corroborating the relevance of the SST threshold for ascending motions (THR)—most likely SST (MLT) index proposed by Bellucci et al. (2010) to explain the double ITCZ bias. However, since atmosphere-only simulations have the same SST forcing, the THR–MLT index measures the atmospheric contribution to this index (i.e., the typical THR) and does not evaluate the role of coupled feedbacks as measured by the MLT. Also, increasing the lateral entrainment reduces the biases in convective versus stratiform precipitation partitioning that have been diagnosed in most current CGCMs (Dai 2006). The error in the precipitation magnitude under strong ascending regimes still persists. Although not frequent, these regimes could be responsible for the remaining errors in the precipitation geographical distribution, particularly the overestimation of precipitation over the west Pacific warm pool. Precipitation magnitude under shallow convective regimes is also overestimated, contributing to the remaining errors in precipitation in large-scale subsiding regions, particularly over the southeastern Pacific Ocean. A special focus on the representation of these particular regimes and the associated precipitation is needed to further improve the tropical precipitation distribution. A possible way to correct this excess of precipitation is to increase rain reevaporation or decrease precipitation efficiency, which both led, in previous AGCM experiments, to the reduction of the double ITCZ bias (Bacmeister et al. 2006; Li et al. 2007).

The comparison between coupled and uncoupled sensitivity simulations shows that the coupled model requires a larger entrainment rate than the atmosphere-only model to produce significant differences in the precipitation patterns. In fact, ocean–atmosphere feedbacks amplify the double ITCZ bias and are responsible for most of its amplitude. As a result, convection inhibition through entrainment needs to be stronger in the coupled model to overcome the amplifying effect of coupled processes. Indeed, this result suggests that

alleviating the double ITCZ bias in the atmospheric models will not be enough to solve the double ITCZ problem in the coupled models. Further improvements in the simulation of ocean–atmosphere interactions will also be necessary to eradicate the double ITCZ bias in coupled models.

Acknowledgments. The authors thank Aurore Voldoire and Sophie Tytecas for their help on the CNRM-CM5. We also thank Isabelle Beau for helpful discussions throughout the course of this work. Thanks are also due to the editor and reviewers for their valuable comments.

REFERENCES

- Adler, R. F., and Coauthors, 2003: The version-2 Global Precipitation Climatology Project (GPCP) monthly precipitation analysis (1979–present). *J. Hydrometeorol.*, **4**, 1147–1167.
- Bacmeister, J. T., M. J. Suarez, and F. R. Robertson, 2006: Rain reevaporation, boundary layer–convection interactions, and Pacific rainfall patterns in an AGCM. *J. Atmos. Sci.*, **63**, 3383–3403.
- Bechtold, P., M. Kohler, T. Jung, F. Doblas-Reyes, M. Leutbecher, M. J. Rodwell, F. Vitart, and G. Balsamo, 2008: Advances in simulating atmospheric variability with the ECMWF model: From synoptic to decadal time-scales. *Quart. J. Roy. Meteor. Soc.*, **134**, 1337–1351.
- Belamari, S., and A. Pirani, 2007: Validation of the optimal heat and momentum fluxes using the ORCA2-LIM global oceanic model. Marine Environment and Security for the European Area-Integrated Project (MERSEA IP) Deliverable D4.1.3, 88 pp.
- Bellon, G., and A. H. Sobel, 2010: Multiple equilibria of the Hadley circulation in an intermediate-complexity axisymmetric model. *J. Climate*, **23**, 1760–1778.
- Bellucci, A., S. Gualdi, and A. Navarra, 2010: The double-ITCZ syndrome in coupled general circulation models: The role of large-scale vertical circulation regimes. *J. Climate*, **23**, 1127–1145.
- Betts, A. K., and M. J. Miller, 1986: A new convective adjustment scheme. Part II: Single column tests using GATE wave, BOMEX, ATEX and arctic air-mass data sets. *Quart. J. Roy. Meteor. Soc.*, **112**, 693–709.
- Bony, S., J. L. Dufresne, H. Le Treut, J. J. Morcrette, and C. Senior, 2004: On dynamic and thermodynamic components of cloud changes. *Climate Dyn.*, **22**, 71–86.
- Bougeault, P., 1985: A simple parameterization of the large-scale effects of cumulus convection. *Mon. Wea. Rev.*, **4**, 469–485.
- Chao, W. C., 2000: Multiple quasi equilibria of the ITCZ and the origin of monsoon onset. *J. Atmos. Sci.*, **57**, 641–651.
- , and B. Chen, 2004: Single and double ITCZ in an aqua-planet model with constant sea surface temperature and solar angle. *Climate Dyn.*, **22**, 447–459.
- Charney, J. G., 1971: Tropical cyclogenesis and the formation of the ITCZ. *Mathematical Problems of Geophysical Fluid Dynamics*, W. H. Reid, Ed., American Mathematical Society, 355–368.
- Chikira, M., 2010: A cumulus parameterization with state-dependent entrainment rate. Part II: Impact on climatology in a general circulation model. *J. Atmos. Sci.*, **67**, 2194–2211.
- , and M. Sugiyama, 2010: A cumulus parameterization with state-dependent entrainment rate. Part I: Description and sensitivity to temperature and humidity profiles. *J. Atmos. Sci.*, **67**, 2171–2193.
- Dai, A. G., 2006: Precipitation characteristics in eighteen coupled climate models. *J. Climate*, **9**, 4605–4630.
- Del Genio, A. D., 2011: Representing the sensitivity of convective cloud systems to tropospheric humidity in general circulation models. *Surv. Geophys.*, **33**, 637–656.
- Déqué, M., C. Dreveton, A. Braun, and D. Cariolle, 1994: The ARPEGE/IFS atmosphere model: A contribution to the French community climate modelling. *Climate Dyn.*, **10**, 249–266.
- Derbyshire, S. H., I. Beau, P. Bechtold, J.-Y. Grandpeix, J.-M. Piriou, J.-L. Redelsperger, and P. M. M. Soares, 2004: Sensitivity of moist convection to environmental humidity. *Quart. J. Roy. Meteor. Soc.*, **130**, 3055–3079.
- Emanuel, K. A., 1991: A scheme for representing cumulus convection in large-scale models. *J. Atmos. Sci.*, **48**, 2313–2329.
- Fouquart, Y., and B. Bonnel, 1980: Computations of solar heating of the earth's atmosphere: A new parametrization. *Contrib. Atmos. Phys.*, **53**, 35–62.
- Frierson, D. M. W., 2007: The dynamics of idealized convection schemes and their effect on the zonally averaged tropical circulation. *J. Atmos. Sci.*, **64**, 1959–1976.
- Gregory, D., and P. R. Rowntree, 1990: A mass flux convection scheme with representation of cloud ensemble characteristics and stability dependent closure. *Mon. Wea. Rev.*, **118**, 1483–1506.
- Hess, P. G., D. S. Battisti, and P. J. Rasch, 1993: Maintenance of the inter-tropical convergence zones and the tropical circulation on a water-covered earth. *J. Atmos. Sci.*, **50**, 691–713.
- Holton, J. R., J. M. Wallace, and J. A. Young, 1971: On boundary layer dynamics and the ITCZ. *J. Atmos. Sci.*, **28**, 275–280.
- Hubert, L. F., A. F. Krueger, and J. S. Winston, 1969: The double intertropical convergence zone—Fact or fiction? *J. Atmos. Sci.*, **26**, 771–773.
- Kuang, Z., and C. S. Bretherton, 2006: A mass flux scheme view of a high-resolution simulation of a transition from shallow to deep cumulus convection. *J. Atmos. Sci.*, **63**, 1895–1909.
- Li, L., B. Wang, Y. Wang, and H. Wan, 2007: Improvements in climate simulation with modifications to the Tiedtke convective parameterization in the grid-point atmospheric model of IAP LASG (GAMIL). *Adv. Atmos. Sci.*, **24**, 323–335.
- Lin, J.-L., 2007: The double-ITCZ problem in IPCC AR4 coupled GCMs: Ocean–atmosphere feedback analysis. *J. Climate*, **20**, 4497–4525.
- Lindzen, R. S., 1974: Wave-CISK in the tropics. *J. Atmos. Sci.*, **31**, 156–179.
- Liu, Y., L. Guo, G. Wu, and Z. Wang, 2010: Sensitivity of ITCZ configuration to cumulus convective parameterizations on an aqua planet. *Climate Dyn.*, **34**, 223–240.
- Louis, J. F., 1979: A parametric model of vertical eddy fluxes in the atmosphere. *Bound.-Layer Meteorol.*, **17**, 187–202.
- Mechoso, C. R., and Coauthors, 1995: The seasonal cycle over the tropical Pacific in coupled ocean–atmosphere general circulation models. *Mon. Wea. Rev.*, **123**, 2825–2838.
- Mlawer, E. J., S. J. Taubman, P. Brown, M. J. Iacono, and S. A. Clough, 1997: Radiative transfer for inhomogeneous atmospheres: RRTM, a validated correlated-*k* model for the longwave. *J. Geophys. Res.*, **102**, 16 663–16 682.
- Neale, R. B., and B. J. Hoskins, 2000: A standard test for AGCMs including their physical parameterizations: I: The proposal. *Atmos. Sci. Lett.*, **1**, 101–107.
- , J. H. Richter, and M. Jochum, 2008: The impact of convection on ENSO: From a delayed oscillator to a series of events. *J. Climate*, **21**, 5904–5924.

- Neggers, R. A. J., J. D. Neelin, and B. Stevens, 2007: Impact mechanisms of shallow cumulus convection on tropical climate dynamics. *J. Climate*, **20**, 2623–2642.
- Noilhan, J., and S. Planton, 1989: A simple parameterization of land surface processes for meteorological models. *Mon. Wea. Rev.*, **117**, 536–549.
- , and J. F. Mahfouf, 1996: The ISBA land surface parameterisation scheme. *Global Planet. Change*, **13**, 145–159.
- Numaguti, A., 1993: Dynamics and energy balance of the Hadley circulation and the tropical precipitation zones: Significance of the distribution of evaporation. *J. Atmos. Sci.*, **50**, 1874–1887.
- , and Y.-Y. Hayashi, 1991: Behavior of cumulus activity and the structures of circulations in an “aqua planet” model. Part II: Eastward-moving planetary scale structure and the intertropical convergence zone. *J. Meteor. Soc. Japan*, **69**, 563–579.
- Oort, A. H., and J. J. Yienger, 1996: Observed interannual variability in the Hadley circulation and its connection to ENSO. *J. Climate*, **9**, 2751–2767.
- Oueslati, B., and G. Bellon, 2013: Tropical precipitation regimes and mechanisms of regime transitions: Contrasting two aqua-planet general circulation models. *Climate Dyn.*, in press.
- Ricard, J. L., and J. F. Royer, 1993: A statistical cloud scheme for use in an AGCM. *Ann. Geophys.*, **11**, 1095–1115.
- Schneider, E. K., 2002: Understanding differences between the equatorial Pacific as simulated by two coupled GCMS. *J. Climate*, **15**, 449–469.
- Smith, R., 1990: A scheme for predicting layer clouds and their water content in a general circulation model. *Quart. J. Roy. Meteor. Soc.*, **116**, 435–460.
- Song, X. L., and G. J. Zhang, 2009: Convection parameterization, tropical Pacific double ITCZ, and upper-ocean biases in the NCAR CCSM3. Part I: Climatology and atmospheric feedback. *J. Climate*, **22**, 4299–4315.
- Sumi, A., 1992: Pattern formation of convective activity over the aqua-planet with globally uniform sea surface temperature (SST). *J. Meteor. Soc. Japan*, **70**, 855–876.
- Terray, L., 1998: Sensitivity of climate drift to atmospheric physical parameterizations in a coupled ocean–atmosphere general circulation model. *J. Climate*, **11**, 1633–1658.
- Volodire, A., and Coauthors, 2013: The CNRM-CM5.1 global climate model: Description and basic evaluation. *Climate Dyn.*, in press.
- Waliser, D. E., and R. C. J. Somerville, 1994: The preferred latitudes of the intertropical convergence zone. *J. Atmos. Sci.*, **51**, 1619–1639.